Controllable Grid Interface for Testing Ancillary Service Controls and Fault Performance of Utility-Scale Wind Power Generation

Preprint

Vahan Gevorgian, Przemyslaw Koralewicz, Robb Wallen, and Eduard Muljadi
National Renewable Energy Laboratory

Presented at the 15th International Workshop on Large-Scale Integration of Wind Power into Power Systems as well as on Transmission Networks for Offshore Wind Power Plants
Vienna, Austria
November 15–17, 2016

NREL is a national laboratory of the U.S. Department of Energy
Office of Energy Efficiency & Renewable Energy
Operated by the Alliance for Sustainable Energy, LLC

This report is available at no cost from the National Renewable Energy Laboratory (NREL) at www.nrel.gov/publications.

Conference Paper
NREL/CP-5D00-67247
February 2017

Contract No. DE-AC36-08GO28308

NOTICE

This report is available at no cost from the National Renewable Energy Laboratory (NREL) at www.nrel.gov/publications.

Available electronically at SciTech Connect http:/www.osti.gov/scitech

Available for a processing fee to U.S. Department of Energy and its contractors, in paper, from:

U.S. Department of Energy
Office of Scientific and Technical Information
P.O. Box 62
Oak Ridge, TN 37831-0062
OSTI http://www.osti.gov
Phone: 865.576.8401
Fax: 865.576.5728
Email: reports@osti.gov

Available for sale to the public, in paper, from:

U.S. Department of Commerce
National Technical Information Service
5301 Shawnee Road
Alexandria, VA 22312
NTIS http://www.ntis.gov
Phone: 800.553.6847 or 703.605.6000
Fax: 703.605.6900
Email: orders@ntis.gov

Cover Photos by Dennis Schroeder: (left to right) NREL 26173, NREL 18302, NREL 19758, NREL 29642, NREL 19795.

NREL prints on paper that contains recycled content.

Controllable Grid Interface for Testing Ancillary Service Controls and Fault Performance of Utility-Scale Wind Power Generation

Vahan Gevorgian, Przemyslaw Koralewicz, Robb Wallen, Eduard Muljadi
National Renewable Energy
Laboratory
Golden, CO, USA

Abstract— **The rapid expansion of wind power has led many transmission system operators (TSOs) to demand modern wind power plants (WPPs) to comply with strict grid interconnection requirements. Such requirements involve various aspects of wind power plant operation, including fault ride-through and power quality performance as well as the provision of ancillary services to enhance grid reliability. During recent years, the National Renewable Energy Laboratory (NREL) of the U.S. Department of Energy has developed a new, ground-breaking testing apparatus and methodology to test and demonstrate many existing and future advanced controls for wind power generation (and other renewable generation technologies) on the multi-MW scale and medium-voltage (MV) levels. This paper describes the capabilities and control features of NREL's 7-MVA power electronic grid simulator (also called a controllable grid interface, or CGI) that enables testing many active and reactive power control features of modern wind turbine generators—including inertial response, primary and secondary frequency responses, and voltage regulation under a controlled medium-voltage grid environment. In particular, this paper focuses on the specifics of testing the balanced and unbalanced fault ride-through characteristics of wind turbine generators under simulated strong and weak MV grid conditions. This paper also describes the test results for some advanced control features, such as wind generation's participation in power system oscillation damping. In addition, the paper provides insights on the power hardware-in-the-loop (PHIL) feature implemented in the CGI to emulate (in real time) the conditions that might exist in various types of power systems under normal operations and/or contingency scenarios. Using actual test examples and simulation results, this paper describes the value of CGI as an ultimate modeling validation tool for all types of "grid-friendly" controls by wind generation.**

Keywords- electric grids; power system faults; power quality; wind energy integration; wind turbine test facilities

I. INTRODUCTION

Power systems throughout the world are undergoing a significant transition from those that are based on large, centralized power plants to more distributed systems that have large numbers of generation units based on renewable energy sources [1]. Integrating high levels of power converter-coupled variable renewable energy resources (wind and solar) into an electric grid requires significant changes to electricity system planning and operations to ensure continued reliability [2]; therefore, it is important to better understand how power-converter-based renewable energy systems interact with the grid and how to utilize the advanced grid-friendly controls by renewables to maintain or enhance grid reliability. Several national and international standards and test procedures ensure that variable renewable technologies can meet the evolving reliability and controllability requirements by grid operators. Manufacturers, developers, and power plant operators of renewable energy systems need to perform series of tests to demonstrate plant operation under grid disturbances and the systems' abilities to provide various types of ancillary services to enhance reliability. For instance, the latest edition of International Electrotechnical Commission Standard (IEC) 61400-21 for power quality testing of utility-scale wind turbine generators provides procedures for low-voltage ride-through (LVRT), active power and frequency responsive controls, and reactive power controls [3]. The newer, in-process edition of the same standard will be setting test requirements for an even larger scope of advanced controls, such as inertial response by wind turbine generators. The performance of converter-coupled generation requires verification at all power ranges under realistic operating conditions. In conventional field-testing, the device under test (DUT) is connected to a specific grid for long periods of time; however, this does not guarantee that the DUT will experience the entire range of possible grid conditions—e.g., frequency variations, balanced or unbalanced voltage fault conditions for testing LVRT or high-voltage ride-through (HVRT) controls—and changing grid characteristics, such as the inertia of the grid and stronger or weaker interconnections.

A first multimegawatt grid simulator of this kind, the controllable grid interface (CGI), was commissioned at the National Wind Technology Center (NWTC) at the National Renewable Energy Laboratory (NREL) in Boulder, Colorado during 2013–2014 [4]. It became the central point of a testing infrastructure that enables the electrical integration testing of various types of renewable energy sources; see Figure 1. This system makes it possible to test devices in fully controllable conditions, including wind turbine nacelles in dynamometer buildings, as well as devices operating on-site: wind turbines, photovoltaic arrays, and energy storage systems. The first results from wind power-related tests conducted with NREL's CGI were demonstrated in [5] and [6], which showed examples of experiments to validate dynamic models of wind

turbine generators and test advanced active power controls by wind power. This paper provides a more in-depth review of the grid simulator's functionality, controls, and emulation of voltage fault and frequency fluctuation conditions that occur in real power systems.

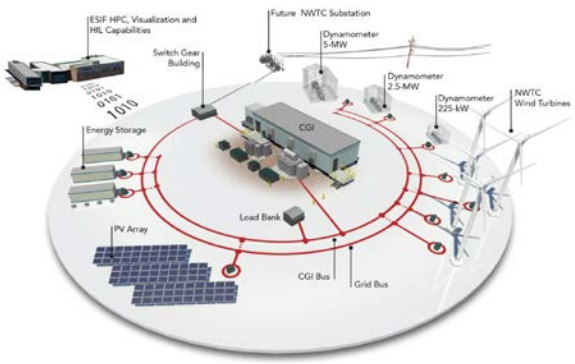

Figure 1. NREL/NWTC infrastructure for renewable energy systems grid integration testing. Illustration by Josh Bauer, NREL

II. Power Converter for Grid Simulator

The unit power capacities of renewable energy systems are increasing. This imposes certain challenges for testing infrastructure because test apparatuses often need to meet more stringent standards than the DUT itself. The continuous power rating of the CGI is 7 MVA. It includes a 9-MVA active line-side rectifier unit that allows power to flow from the DUT to the steady grid with a controllable power factor; however, the test-side converter faces many challenges because it needs to provide grid simulator functionality and maintain full controllability under transient conditions that may exist at the point of common coupling (PCC). Transient overcurrent capability is one important feature of the grid simulator because certain types of generators under test can inject high short-circuit currents that exceed their nominal rating multiple times [7]. For example, a wind turbine that uses a doubly-fed induction generator (DFIG) topology can produce currents up to ten times stronger than its nominal rating under zero-voltage conditions for short time periods [8]; therefore, substantial short-term overcurrent capacity is needed by the grid simulator to maintain stable operation during such transient events. For this purpose, the CGI topology is based on four 3.3-kV medium-voltage, neutral-point-clamped (NPC) inverter units that are normally used to drive industrial-grade motors and a custom step-up transformer to produce 13.2 kV on the test article terminals, as shown in**.** Under continuous 7-MVA operation, the amplitude of the nominal continuous current at the inverter side of the transformer is at 500A. To allow for a significant overcurrent capability, the selected medium-voltage NPC inverters are based on integrated gate-commutated thyristor (IGCT) devices. Their maximum current is 2.7 kA, which allows for a 540% overcurrent margin assuming a 7-MVA DUT.

The custom transformer is designed to match DUTs with various nominal voltages by utilizing multiple transformer taps. The transformer is rated for 7-MVA continuous operation and 560% short-term overcurrent operation to handle short-circuit currents that may be produced by the test articles. The special configuration of the transformer allows synthesizing 17-level low-distortion voltage waveforms by interleaving 3-level phase voltages.

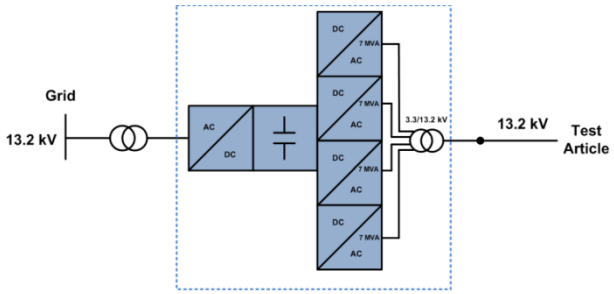

Figure 2. CGI block diagram

For a given semiconductor device, the power capacity can be increased by decreasing the switching frequency, which in turn can lead to voltage quality degradation, which is normally measured as total harmonic distortion (THD). Normally, the desired THD level in power converters can be maintained by a harmonic filter; however, filters also decrease the dynamic range of operation. To maintain dynamic performance as fast as possible, the CGI uses advanced modulation control methods rather than a hardware filter. Thus, a balance is found among three conflicting requirements of power conversion: multimegawatt power ratings, sub-1% THD, and extremely fast response times, typically smaller than 1 ms.

III. PWM Modulation Scheme

The CGI supports two multilevel modulation schemes, each optimized for different objectives. A pulse-width modulated (PWM) scheme is used for highly dynamic operation, and an optimized pulse pattern (OPP) modulator is used to achieve minimum line-to-line voltage THD levels. It is possible to transition from one mode to another during operation; therefore, advanced test scenarios utilizing high power quality in normal operation and high dynamic response during faults can be implemented. This paper describes both modulation techniques that are used to achieve high-quality voltage waveforms utilizing a relatively low switching frequency of the IGCT devices of less than 500 Hz.

A. PWM Modulation

This modulation mode is based on multilevel PWM with eight-level shifted carriers (), allowing high-quality voltage waveforms with fast voltage dynamics. An example of a measured line-to-line voltage waveform with harmonic spectrum is shown in. The voltage THD measured on the line-to-line voltage is less than 5% (calculated up to the 50th harmonic order, as specified in) for the wide range of nominal voltage, from 65%–105%, as shown in a. The PWM modulator gives the best dynamic performance because the reference voltage is compared and updated after every half cycle of multilevel carrier. Due to the utilization of multiple slow-switching NPC stacks, it is possible to use a high, 3,360-Hz carrier frequency. At 60-Hz operation, this results in switching band harmonics that are above the 50th harmonic order. Apart from the high dynamics, the PWM modulator ensures precise and uniform accuracy of the fundamental voltage amplitude. Using advanced calibration techniques, it is possible to achieve less than 0.5% amplitude accuracy.

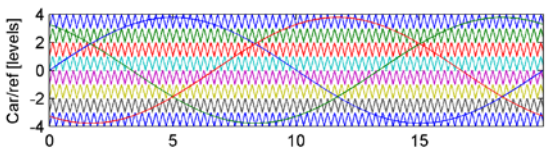

Figure 3. PWM modulation scheme

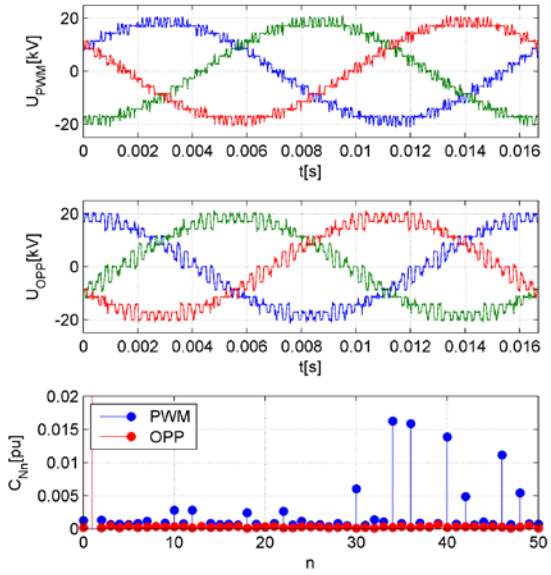

Figure 4. Voltage waveforms at PWM and OPP modulation

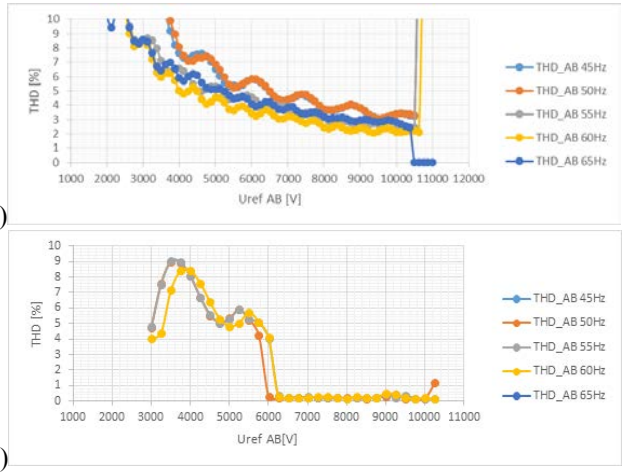

Figure 2. Voltage THD depending on reference voltage at different frequencies: a) PWM mode, b) OPP mode

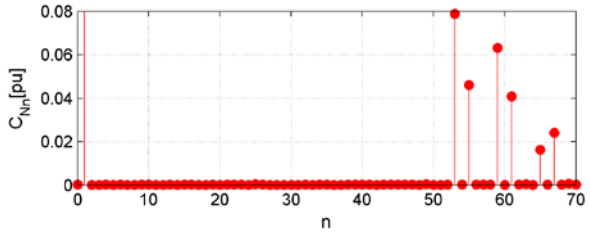

Figure 3. Spectrum of OPP mode up to 70th harmonic

B. *Optimized Pulse Pattern Modulation*

Very low THD levels (less than 1%) within a certain frequency band, up to the 50th harmonic, with low switching frequency for semiconductor devices can be achieved by utilizing sophisticated mathematical methods for harmonic elimination by shifting the harmonic components to higher frequency bands. The modulation patterns are pre-calculated and optimized to reach this goal. An example of a measured voltage waveform with harmonic spectrum is shown in. The OPP results in nearly 0% THD for a wide range of reference voltages—more than 60% of nominal; see b. The fundamental voltage is accurately tracking the reference with <0.5% accuracy, similar to the PWM.

Because the CGI is built using switching devices with no hardware filter, all known limitations of harmonic control are present in the existing design; however, with OPPs the harmonic content can be controlled in a frequency range, but due to the so-called water-bed effect, the harmonic energy is shifting to the uncontrolled bands, as shown in.

Table 1 compares measured voltage THD (including the first 50 harmonics) to the of the fundamental component for both PWM and OPP modulation.

TABLE I. STEADY-STATE THD AND FIRST HARMONIC MEASUREMENTS

Measurement	PWM	OPP
THD50 (%)	3.0639	0.39832
U1 (kV)	13.1055	13.0908

IV. LVRT AND HVRT TESTING USING GRID SIMULATOR

LVRT and HVRT testing is usually done according to voltage drop profiles defined in the specific test scenario or according to the relevant grid code requirements similar to those shown in. The CGI by its design does not contain preprogrammed voltage profiles; instead, it is designed as a voltage amplifier that follows a reference set point from the supervisory controller with a certain dynamic and static tolerance so that any desired voltage profile can be emulated (). This approach allows for great flexibility when designing test profiles. An example waveform of a 100-ms zero-voltage event achieved using the grid simulator without the DUT connected is shown in. More details about the dynamics of the system and its limitations can be found in.

As mentioned earlier, one important aspect of voltage fault performance of some wind turbine generator topologies is their ability to produce large short-circuit currents during the voltage faults. The magnitude of the short-circuit current depends on the wind turbine's electrical topology. High short-circuit currents represent a certain challenge for the grid simulator design because it should be able to absorb such high reactive currents without damaging its power electronics and other converters. For this purpose, NREL's grid simulator was designed to handle currents with magnitudes almost six times that of the rated current. In addition, nonsymmetrical faults create additional challenges in the form of large active and reactive power oscillations. The grid simulator must be designed to provide stable voltage performance in the presence of such oscillations.

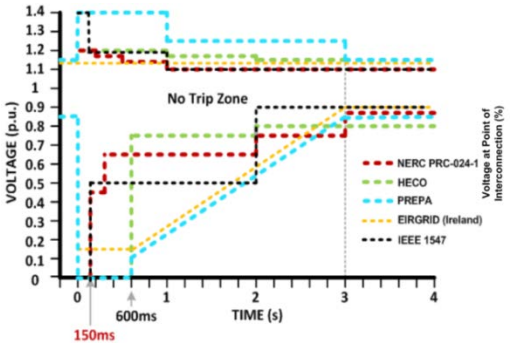

Figure 4. Examples of LVRT/HVRT requirements

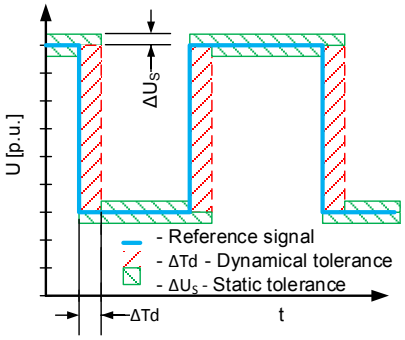

Figure 5. Dynamic tolerance limits of grid simulator

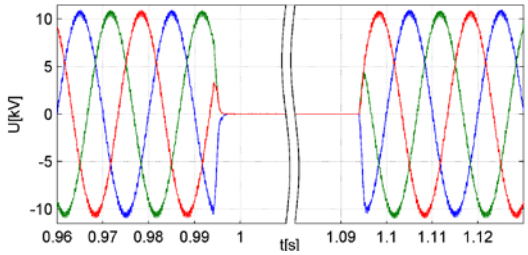

Figure 6. No-load 100-ms zero-voltage fault profile measured at PCC

A number of LVRT and HVRT tests were conducted on a 2.75-MW wind turbine drivetrain, which was installed on NREL's 5-MW dynamometer and connected to the CGI (Figure 10). These tests were conducted when the wind turbine was operating at different power levels (capacities from 0%–100%). The wind turbine under test utilizes a full power converter topology (often referred to as Type 4 topology) coupled with a permanent magnet synchronous generator and a three-stage gearbox. This topology is not prone to producing high short-circuit currents because the generator is fully decoupled from the grid. This is unlike some other wind turbine topologies, such as a DFIG topology, or Type 3, which can produce large short circuit currents. The example results of some symmetrical and nonsymmetrical zero-voltage fault tests when the turbine was operating at rated power are shown in Figure 11 and Figure 12, respectively. In both cases, the CGI was commanded to emulate a 100-ms self-recovering voltage fault that typically takes place in power systems. During both tests, the wind turbine resumed its prefault production after normal voltage conditions were restored. The CGI demonstrated stable operation under both balanced and unbalanced voltage conditions following the commanded voltage profiles.

Figure 7. 2.75-MW WTG drivetrain under test

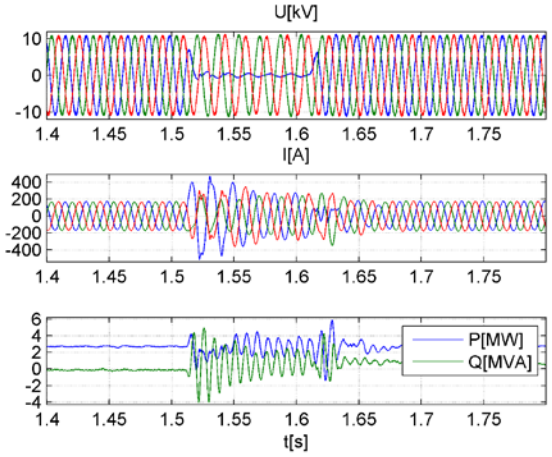

Figure 8. Single-phase zero-voltage test

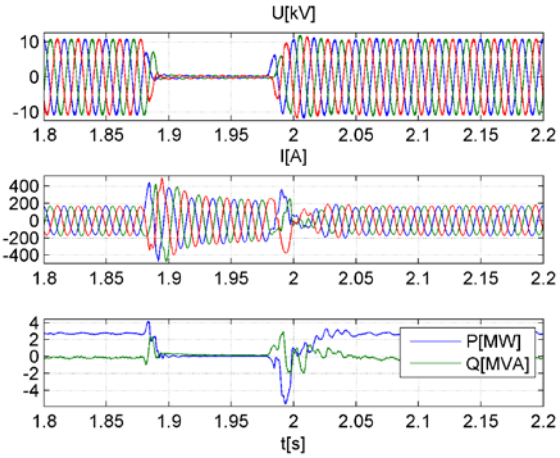

Figure 9. Three-phase zero-voltage test

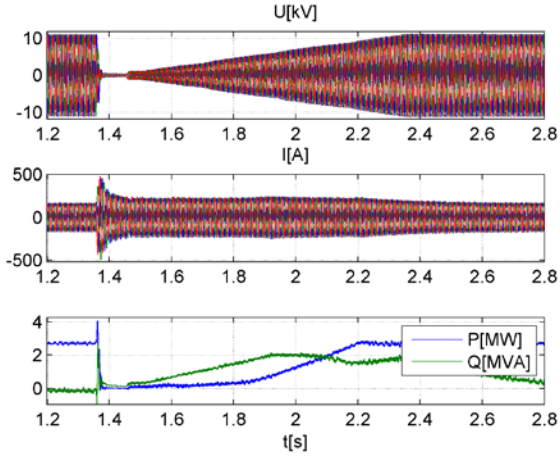

Figure 10. Testing three-phase LVRT profile

Another case, shown in Figure 13, depicts the turbine's reaction to a three-phase LVRT event with slow voltage recovery realized using a 1-s ramp. The DUT continued to deliver reactive current to the system while trying to assist in the PCC voltage recovery. Active power ramped up along with the voltage, and the turbine resumed its prefault production level at t=2.4 s.

A number of 130% symmetrical and nonsymmetrical high-voltage tests also demonstrated stable operation of the CGI. One example of such a test is shown in Figure 14, wherein a 130% three-phase overvoltage event was emulated by the CGI for 100 ms. The wind turbine rode through this condition and resumed its prefault production after the voltage recovery. The CGI provided stable voltage operation during the whole test in accordance with the commanded profile.

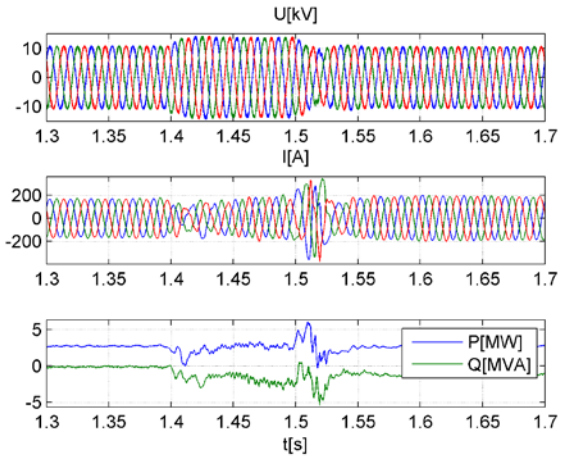

Figure 11. High-voltage test

V. Testing Frequency Responsive Controls Using Grid Simulator

The ability of a power system to maintain its electrical frequency within a safe range is crucial for stability and reliability [14] [15]. An IEEE task force report studied this issue with great detail and developed a number of conclusions and recommendations, including those on the importance of wind generation to provide primary frequency response (PFR) to prevent future declines in the frequency response of the U.S. interconnections [16]. From this perspective, the ability of the power electronic grid simulator to emulate various types of frequency profiles allows testing such controls by emulating realistic frequency events that can occur in any power system for both 50-Hz and 60-Hz grids. One example of this type of test is shown in Figure 15, when the grid simulator was commanded to emulate a real frequency event time series that was measured by NREL in the U.S. Western Interconnection. Such events are typical in power systems and caused by the loss of a large generator due to a temporary imbalance between generation and load. The PFR of conventional generators responds to such events immediately after the frequency decline has passed beyond their governor dead-band thresholds. In this case, the wind turbine under test provided a similar response with 5% frequency droop setting when operating at lower power so that it had enough headroom for up-regulation. As shown in, the wind turbine increased its power output in accordance with the droop setting after the frequency decline exceeded the preset dead band. Similar tests were conducted for overfrequency events as well.

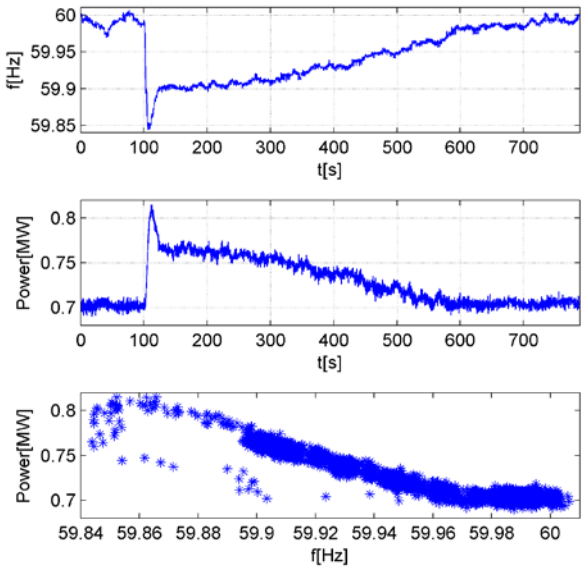

Figure 15. Frequency droop test

The CGI was utilized to test advanced active power controls by wind turbines for power oscillation damping (POD). Such oscillations may exist in power systems under certain conditions. This particular testing is described in great detail in. One example of a POD controls test on a real wind turbine generator is shown in, which compares test data and modeling results. This particular test illustrates another value of the grid simulator as a platform for DUT model validation.

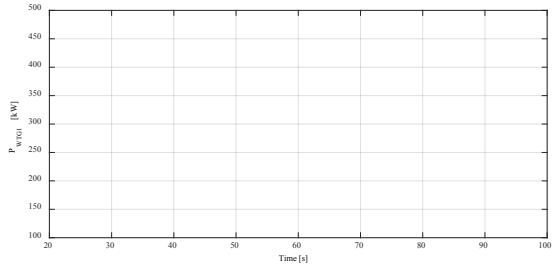

Figure 12. POD test results

VI. Power Hardware-in-the-Loop Capability

Tests described in previous sections utilized predefined patterns of voltage or frequency (open-loop tests). This approach is normally sufficient for testing a particular functionality of power converters; however it neglects the impact of currents being injected onto a power system's voltage and frequency. This type of impact can be a significant factor when operating renewable energy generation connected to weaker grids, so it is important to account for the DUT current impact when testing under simulated grid conditions. Therefore, a closed-loop setup is necessary to a) test the reliable operation of a power system with the DUT providing various types of ancillary services and fault performance and b) identify any undesirable stability issues in the form of interactions between various parts of the power system, such

as frequency instability and oscillations or subsynchronous voltage oscillations. For this purpose, a power hardware-in-the-loop (PHIL) capability was developed for the CGI utilizing the real-time digital simulator (RTDS) system. The PHIL setup allows for conducting experiments with a real generator and for testing its controls with the real-time models of various power systems realized in RTDS. A simplified diagram of the existing PHIL setup is shown in Figure 17.

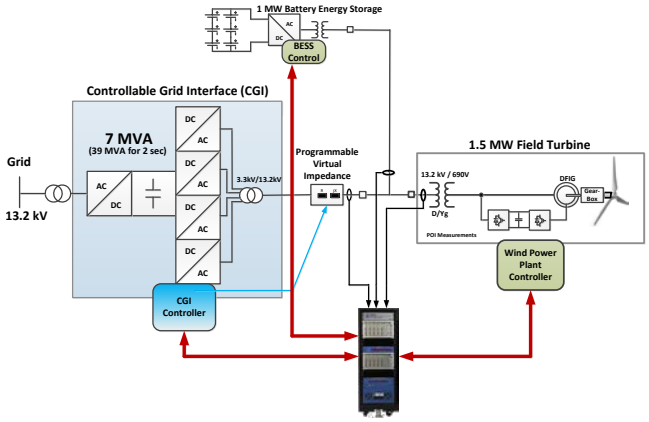

Figure 17. PHIL test setup with CGI and RTDS

Certain power plants or groups of power plants selected from the model can be replaced with any real device available at the NWTC site, including wind turbines in the field and dynamometers, battery storage, etc. The RTDS communications interface allows commanding CGI frequency and voltage set points according to the state of a real-time model running in RTDS. At the same time, actual current response is measured at the PCC and communicated back to RTDS where the current is being injected into the modeled grid. A standard nine-bus IEEE test case has been modified and implemented in RTDS to test frequency responsive controls by wind generation (). An example result of a closed-loop PHIL frequency test realized with the nine-bus test system is shown in, which shows a very close match between the commanded and measured frequency during the generation and load-loss events triggered in the model. These are the initial results of testing to demonstrate the CGI PHIL capability. Another publication that is in progress will provide detailed information on such PHIL tests.

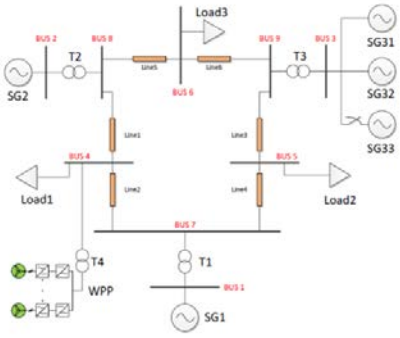

Figure 18. RTDS model of nine-bus power system

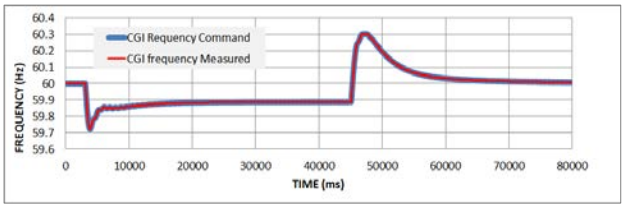

Figure 19. Time series of simulated frequency on CGI terminals

Results of measured inertial responses by a real 1.5 MW wind turbine connected to CGI terminals exposed to the same frequency profile emulated by PHIL/RTDS is shown in. These inertial responses were produced by the wind turbine under various grid conditions, so the profile of each individual response is highly depending of initial turbine conditions (wind speed, power level, rotational speed) at the beginning of underfrequency event. In this case, CGI also appears to be an extremely useful tool for measuring inertial controls by wind power under real frequency conditions when the whole turbine (including its auxiliary equipment) is exposed the real frequency variations.

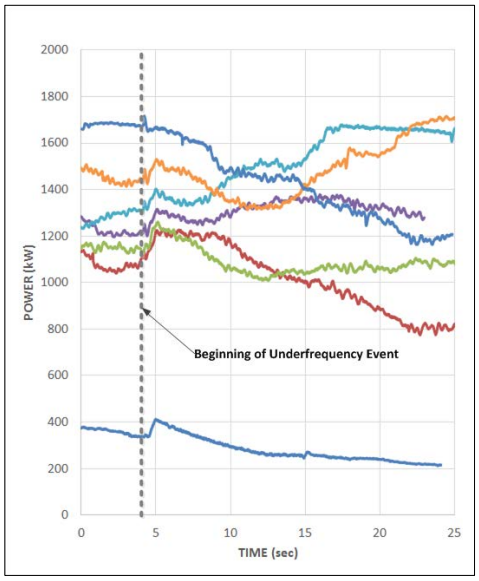

Figure 20. Measured inertial responses by 1.5 MW wind turbine

VII. Virtual Grid Impedance Control

The electrical characteristics of the grid, such as line impedance and short-circuit ratio at the PCC, might impact the ability of inverter-coupled generation to ride through various types of voltage faults and other transient conditions. For example, some wind turbine electrical topologies such as DFIGs need to absorb reactive power from the grid for magnetization, which may deteriorate weak grids. During voltage faults, wind turbines, photovoltaic, and energy storage inverters are capable of supplying reactive current to weak grids to increase the grid voltage and assist with recovery. Also, inverter-coupled generators can provide voltage, reactive power, or power factor control to enhance stability.

A. *Short-Circuit Power and Impedance of Matching Transformer*

With simplifications, the CGI can be viewed as an ideal voltage source inverter with a series impedance of the matching transformer; therefore, the transformer impedance has a significant impact on the parameters of the emulated grid. A short-circuit power (S_{SC}) that allows for the evaluation of grid strength can be estimated using (1):

$$S_{SC} = \frac{U_N}{Z_t} = \frac{S_N}{Z_{tPU}} \qquad (1)$$

The impedance of the CGI transformer $Z_{PU} = 5\%$ for 50-Hz operation and 6% for 60-Hz operation; therefore, the short-circuit ratio of the emulated grid S_{SC} is 20 or 16.66 times higher than the nominal power of grid simulator (S_N) for 50 Hz an 60 Hz, respectively ($S_{SC} = 140\ MVA$ at 50 Hz and 116 MVA at 60 Hz). This value is significantly higher than the rating of any DUT, so the CGI naturally emulates a strong grid interconnection. Note that the impedance of the emulated grid can be accurately estimated at any frequency, making it a useful feature when analyzing the transients with current waveforms consisting of any harmonic or subharmonic components.

B. *Programmable Impedance at Reference Frequency*

To test the DUT's performance under emulated strong and weak grid conditions, a programmable line impedance feature has been implemented in the CGI's controls. The impedance control is implemented for the reference frequency, and it allows for a) compensating the transformer impedance, Z_t, and b) introducing an additional impedance, Z_D. Depending on the commanded reference voltage, U_{Ref}, the controller sets the impedance value, so the voltage at the PCC follows Eq. (2), whereas in reality it is the sum of the inverter voltage and voltage drop of the transformer, as indicated in Eq. (3):

$$\overline{U_{PCC}} = \overline{U_{Ref}} + \overline{Z_d}\bar{I} \qquad (2)$$

$$\overline{U_{PCC}} = \overline{U_{INV}} + \overline{Z_t}\bar{I} \qquad (3)$$

To ensure that the CGI emulates the requested impedance, a voltage vector is generated by the inverter based on equation (4):

$$\overline{U_{INV}} = \overline{U_{Ref}} + (\overline{Z_d} - \overline{Z_t})\bar{I} \qquad (4)$$

The CGI controller calculates the output current vector in real time and modifies the inverter voltage by adding an equivalent of voltage drop on the requested impedance and negative transformer impedance. This way, the CGI can emulate any impedance requested. If zero impedance is requested, the SGI will act as a strong grid because only the transformer voltage drop will be compensated.

The impedance control is implemented in the CGI's hardware-in-the-loop (HIL) emulator. shows the CGI voltage measured at the 13.2-kV PCC for different levels of reactive power injected at three different impedance settings. A case with transformer-only compensation (green trace) corresponds to $S_{SC} = 5118$ MVA, which can be considered nearly infinite compared to the nominal rating of 7 MVA. Other cases for $Z_{dPU} = 6\%\ and\ Z_{dPU} = 10\%$ are shown in red and blue, respectively. Measured S_{SC} values in show that grid impedance can be controlled with sufficient accuracy.

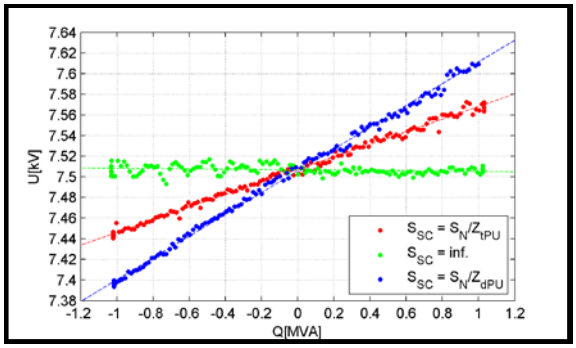

Figure 21. Impedance compensation results using HIL emulation

TABLE II. GRID IIMPEDANCE CONTROL MEASUREMENTS

Impedance Setting	Expected S_{sc}	Measured S_{sc}
$Z_{PU} = Z_{tPU} = 6\%$	116 MVA	123 MVA
$Z_{PU} = Z_{dPU} = 0\%$	inf	-5,118 MVA
$Z_{PU} = Z_{dPU} = 10\%$	70 MVA	71.1 MVA

Test results shown in demonstrate the voltage measured at the terminals of a 1.5-MW fuel cell inverter connected to the CGI. The CGI was set to operate without transformer compensation, and the inverter under test was set to absorb or inject reactive power to modify the voltage at the virtual PCC in accordance with the 5% transformer impedance. As shown in, grid simulator voltage changed linearly with the reactive power at two different voltage levels, with a transition from one voltage level to another. With the transformer compensation enabled, the grid simulator will operate as a stiff voltage source with infinite short-circuit power (S_{SC}.).

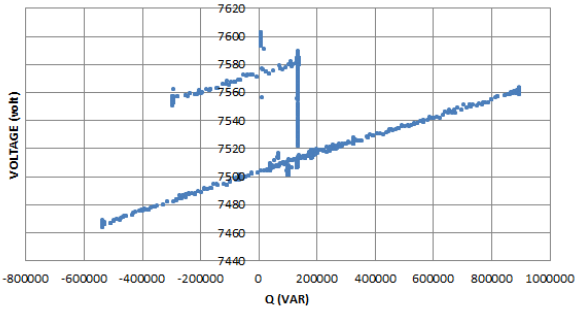

Figure 22. CGI impedance measurements using 1.5-medium-voltage fuel cell inverter

VIII. CONCLUSIONS

This paper presented the capabilities of NREL's 7-MVA power electronic grid simulator to test large, utility-scale wind turbine generators. This grid simulator facility is an advanced and flexible tool for testing many grid integration controls of wind and other renewable generation technologies under controlled medium-voltage grid conditions, and it can be used for both research and certification purposes. The grid voltage fault ride-through testing of wind turbine generators and other technologies is one fundamental benefit of this grid simulator

facility due its ability to emulate low-, zero-, and high-voltage faults of any desired profiles and allow for testing to any grid codes and interconnection requirements for both 50-Hz and 60-Hz systems. Another fundamental benefit of the facility is its ability to emulate frequency deviations that can happen in any power system, thus enabling testing of advanced frequency responsive controls by renewable generation. Over- and underfrequency events that happen periodically in power systems can be replicated on the grid simulator terminals many times, so inertial and PFR controls by renewable generators can be tested and tuned to the requirements of any system operator. Another important ability of the grid simulator is the programmable (virtual) impedance control, which allows for emulation of "strong" and "weak" grid interconnection conditions. The results demonstrated in this paper are unique and clearly show the value of the NREL's power electronic grid simulator for testing advanced grid-friendly controls of renewable generation.

IX. Acknowledgments

This work was supported by DOE under Contract No. DE-AC36-08GO28308 with NREL. Funding provided by U.S. DOE Office of Energy Efficiency and Renewable Energy Wind Program. The authors would also like to thank Mr. Xiao Wang of University of Denver; ABB Corporate Research Center in Krakow, Poland; and ABB MV Drives Division in Turgi, Switzerland for their continuous support of this work.

References

[1] P. Sullivan, W. Cole, N. Blair, and E. Lantz, 2015 Standard Scenarios Annual Report: U.S. Electric Sector Scenario Exploration (NREL/TP-6A20-64072). Golden, CO: July 2015.

[2] North American Electric Reliability Corporation, 2013 Special Reliability Assessment: Maintaining Bulk Power System Reliability while Integrating Variable Energy Resources. Washington, DC: November 2013.

[3] International Electrotechnical Commission, IEC 61400-21, Edition 2, "Measurement and Assessment of Power Quality Characteristics of Grid-Connected Wind Turbines," 2008.

[4] V. Gevorgian, R. Wallen, and M. McDade, "NREL controllable grid interface for testing of renewable energy technologies (paper presented at the 3rd International Workshop on Grid Simulator Testing, Tallahassee, TN, November 2015).

[5] L. Zeni, P. E. Sorensen, A. D. Hansen, B. Hesselbaek, and P. C. Kjaer, Power System Integration of VSC-HVDC Connected Offshore Wind Power Plants. Kongens Lyngby, Denmark: Technical Unioversity of Denmark/DONG Energy, July 2015.

[6] L. Zeni, V. Gevorgian, R. Wallen, J. Bech, P. E. Sorensen, and B. Hesselbaek, "Utilization of real-scale renewable energy test facility for validation of generic wind turbine and wind power plant controller models," IET Renewable Power Generation, May 2016.

[7] E. Muljadi and V. Gevorgian "Short-circuit modeling of a wind power plant" (paper presented at the 2011 IEEE PES GM, Detroit, MI, July 24–28).

[8] J. Morren and S. W. H. de Haan, "Short-circuit current of wind turbines with doubly fed induction generator," IEEE Trans. Energy Convers., vol. 20, June 2005.

[9] P. Steimer, O. Apeldoorn, and E. Carroll, "Igct devices-applications and future opportunities," IEEE Power Engineering Society Summer Meeting, vol. 2, pp. 1,223–1,228, 2000.

[10] U.S. Federal Energy Regulatory Commission, Order 661-A, "Interconnection of Wind Energy," December 2005.

[11] IEEE, Standard 519-2014, "Recommended Practice and Requirements for Harmonic Control in Electric Power Systems," 2014.

[12] P. Koralewicz, V. Gevorgian, R. Wallen, W. van der Merwe, and P. Jörg, "Advanced grid simulator for multi-megawatt power converter testing and certification" (paper presented at the 2016 IEEE ECCE, Milwaukee, WI, September 18–22).

[13] E. Muljadi, N. Samaan, V. Gevorgian, J. Li, and S. Pasupulat, "," IEEE Trans., Industry Appl., vol. 49, pp. 264–292, January 2013.

[14] V. Gevorgian, Y. Zhang, and E. Ela, "," IEEE Trans. Sustain. Energy, vol. 6, no. 3, pp. 1,004–1,012, July 2015.

[15] P. Du amd N. Lu, Energy Storage for Smart Grids. Elsevier: 2014, Chapter 4, pp. 97–113.

[16] IEEE Task Force on Large Interconnected Power Systems Response to Generation Governing, "Interconnected power system response to generation governing: Present practice and outstanding concerns," IEEE Special Publication 07TP180, May 2007.

[17] S. Chandrasekaran, C. Rossi, and D. Casadei, "Improved control strategy for LVRT capability of DFIG with grid code requirements," Electrical and Computer Engineering: An International Journal (ECIJ), vol. 2, no. 2, June 2013.

[18] A. J. Wood, B. F. Wollenberg, and G. B. Sheble, G.B. Power Generation, Operation and Control, Third Edition. Hoboken, NJ: John Wiley and Sons, 2014.

[19] L. Zeni, V. Gevorgian, et.al., "Utilization of real-scale renewable energy test facitlity for validation of generic wijd turbine and wind power plant controller models," IET Renewable Power Generation, 2016.